

A PROGRESSIVE DAMAGE MODEL FOR BOLTED JOINTS IN THREE-DIMENSIONAL WOVEN CARBON COMPOSITES SUBJECTED TO SINGLE-BOLT, DOUBLE-SHEAR LOADING

Kyle Warren¹, Harun Bayraktar¹, Roberto Lopez-Anido², Senthil Vel³

¹Albany Engineered Composites
Research, Technology and Development
112 Airport Drive, Rochester, NH 03867, USA
kyle.warren@albint.com
harun.bayraktar@albint.com
<http://www.albint.com/aec>

²Advanced Structures and Composites Center
University of Maine, 35 Flagstaff Road, Orono, ME 04469, USA
rla@maine.edu
<http://composites.umaine.edu/>

³Mechanical Engineering Department
University of Maine, 5711 Boardman Hall, Orono, ME 04469, USA
senthil.vel@maine.edu
<http://umaine.edu/mecheng/>

Keywords: 3D woven, joining, progressive damage, simulation, bolted joints

Abstract

Three-dimensional woven composite materials provide unique advantages when compared with traditional two-dimensional fiber reinforcement, including enhanced through-thickness performance and elimination of delamination as a possible material failure mode. To extend the understanding of and applications for these materials, a single-bolt, double-shear joint has been studied using an implicit finite element model in Abaqus to predict the onset and initial propagation of damage at the constituent material level. To achieve this, a progressive damage model has been developed and applied to a voxelized finite element discretization of impregnated tow and matrix material phases at the mesoscale. Far from the bearing area, orthotropic material properties are assigned at the composite-level to describe the macroscale. This imperfect as-molded fiber reinforcement in the mesoscale geometry represents a layer to layer angle interlock three-dimensional woven architecture with 24K IM7 carbon tows and PR520 toughened epoxy resin. Damage is applied to the mesoscale through the degradation of compliances using the Matzenmiller-Lubliner-Taylor damage model with Hashin failure criteria applied to the transversely isotropic carbon tows and a maximum principal stress criteria for matrix degradation. Simulation results were found to exhibit trends seen in published experimental findings from previous work for the bolted joint of interest. This good agreement between simulation and experimental results supports the adopted approach for progressive damage modeling to study the onset of damage within the mesoscale for this fiber architecture.

1. Introduction

This paper is focused on exploring the failure modes and damage characteristics of a layer to layer interlocked three-dimensional woven composite in a double-shear bolted joint configuration through finite element simulation with progressive failure. Three-dimensional woven composites are currently used in the Leading Edge Aviation Propulsion (LEAP) engine platform by CFM International for both fan blade and fan case applications. Similar three-dimensional woven composites have also been used for landing gear braces for the Boeing 787-8 Dreamliner and the LiftFan for the F-35 Lightning II jet. Three-dimensional woven composites have been found to reduce part cost, touch labor and even consume less material than traditional laminated composites by leveraging near net-shape preforming [1].

Progressive damage modeling of three-dimensional woven composites is a relatively new research area. Research efforts have previously focused on the development of progressive damage models (PDM) applied to two-dimensional composites [2, 3] and three-dimensional woven composites in general [4]. Combining both damage modeling and bolted joints, Camanho and Matthews developed stiffness degradation factors to capture damage in two-dimensional composites [5]. Similar research work has focused on the effect of bolt hole clearance on the performance of traditional laminated composites for aerospace applications during the Bolted Joints in Composites Aircraft Structures (BOJCAS) project [6]. Simulation results from this project agreed with experimental findings in that as the clearance around a single bolt in single-shear hole became larger, a reduction in joint stiffness resulted.

The understanding of the onset of failure and contributing failure mechanisms in composites with three-dimensional woven fiber reinforcement is necessary for rapid design and evaluation of new components. This paper discusses the development of a first-pass PDM for a notched 3D woven composite part subjected to a single-bolt, double-shear load and compares simulation results with previous experimental findings. Many of the intricacies in the approach described herein are beyond the scope of this paper and are discussed in more detail in Ref. [7].

2. Simulation Approach and Methods

This paper explores the material response of an aerospace-grade carbon/epoxy composite with three-dimensional woven fiber reinforcement. The geometry of interest is a single bolt fastened joint loaded in a double lap shear configuration and experimentally evaluated following ASTM D5961, Procedure A [8]. A progressive damage model is needed to capture the initial onset and propagation of damage within this joint. A multiscale model was developed where the 3D woven composite is assumed to have orthotropic behavior far away from the bolt. Closer to the area of interest, a mesoscale modeling approach is applied where both matrix and impregnated tow material are discretely defined to form the 'as-molded' composite geometry. A diagram of the model dimensions, boundary conditions and material phase locations is found in Figure 1. Fully-integrated C3D8 continuum 'brick' elements were used in the mesoscale and C3D8R elements were used in the orthotropic region far from the hole with reduced-integration.

Simulation of material degradation and progressive failure requires multiple components including failure criteria to establish when a material is predicted to fail and a constitutive damage model that degrades material properties to represent physical damage and failure. Additionally, a damage evolution law is needed to describe how the failure criteria are applied to the damage model (instantaneous damage, exponential, power, etc). Reference material orientations and stress components described in this paper refer to a mutually orthogonal right coordinate system where the 1-direction is oriented coincident with the fiber direction within a tow and the 2-3 plane is a plane of isotropy (i.e. transversely isotropic).

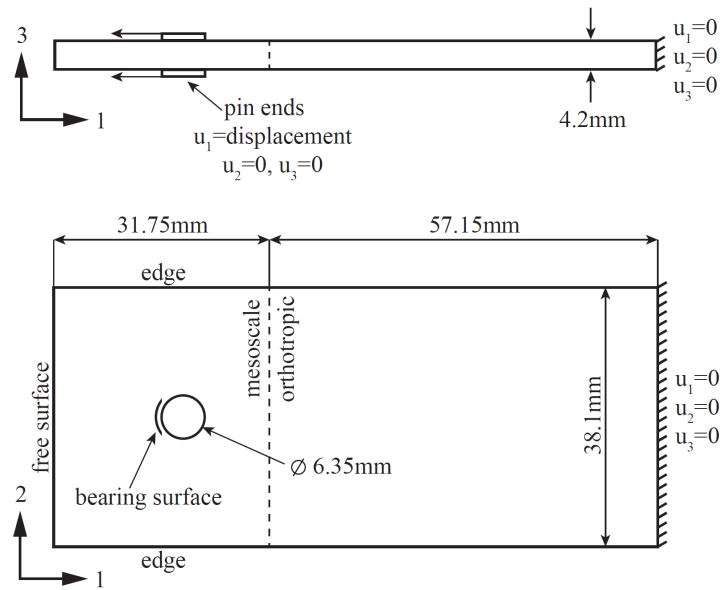


Figure 1. Model geometry, boundary conditions and material phase location definition

3. Materials

The simulation work described in this paper is focused on the mechanical performance of a composite reinforced with a three-dimensional (3D) woven preform. This layer to layer interlocked preform was woven on a specialized Jacquard loom with IM7 carbon fiber. The dry fiber preform was then injected with Cycom PR520, a toughened aerospace epoxy resin system, using a resin transfer molding (RTM) process. A representative volume element (RVE) of this 3D woven pattern encompasses four pick columns and four warp columns (4x4), measuring nominally 10.2 mm × 10.2 mm. The 3D woven architecture explored in this paper is evaluated in tension, compression and shear in Ref. [9] and in bearing in Ref. [10]. Matrix properties used as model inputs are found in Table 1. Impregnated tow elastic properties are listed in Table 2 and corresponding impregnated tow strengths are found in Table 3. Impregnated tow properties were determined using experimental methods described in Ref. [7].

Table 1. Isotropic epoxy matrix properties (PR-520) [11]

Property	Symbol	Value
Elastic Modulus (GPa)	E	4.00
Poisson's Ratio	ν	0.398
Tensile Strength (MPa)	Y_T	82.1
Compressive Strength (MPa)	Y_C	128
Shear Strength (MPa)	τ_{ult}	61.4

3.1. Failure Criteria, Failure Indicators and Damage Variables

Hashin failure criteria was selected for the impregnated tow material phase within the mesoscale because it is commonly applied to composite materials and can capture transversely isotropic material behavior [12]. Additionally, it has been shown to be effective in composite bolted joints [5, 13, 14]. The value of

Table 2. Impregnated tow elastic material properties [7]

Elastic Properties	
E_1	180 GPa
$E_2 = E_3$	9.45 GPa
$\nu_{12} = \nu_{13}$	0.433
ν_{23}	0.465
$G_{12} = G_{13}$	6.67 GPa
G_{23}	3.23 GPa

Table 3. Impregnated tow strength properties [7]

Strength Parameter (direction)	Symbol	Strength (MPa)
Longitudinal Tensile (1)	S_1^T	1810
Longitudinal Compressive (1)	S_1^C	669
Transverse Tensile (2, 3)	$S_2^T = S_3^T$	64.0
Transverse Compressive (2, 3)	$S_2^C = S_3^C$	174
Shear (1-2,1-3)	$S_{12}^F = S_{13}^F$	105
Shear (2-3)	S_{23}^F	105

each failure indicator (f_1, f_2, f_3 and f_4) is evaluated by solving $F(\sigma/f) = 1$ (where σ is the stress tensor) using the respective equation in Table 4. It should be noted that when f_3 and f_4 , the two matrix-mode failure indicators, refer to σ_{22} and σ_{33} , they are referencing the principal stresses within the 2-3 plane of isotropy. The Matzenmiller-Lubliner-Taylor (MLT) constitutive damage model [15] was adopted for this simulation. Using MLT, the compliance matrix is evaluated at each material point as a function of damage variables d_1, d_2, d_3 , and d_4 and is shown in Equation 1.

Table 4. Hashin failure criteria [12]

Failure Mode and Condition	Failure Criteria
Tensile Fiber $\sigma_{11} > 0$	$F_1(\sigma) = \left(\frac{\sigma_{11}}{S_1^T}\right)^2 + \frac{1}{(S_{12}^F)^2} (\sigma_{12}^2 + \sigma_{13}^2) = 1$
Compressive Fiber $\sigma_{11} < 0$	$F_2(\sigma) = \frac{-\sigma_{11}}{S_1^C} = 1$
Tensile Matrix $\sigma_{22} + \sigma_{33} > 0$	$F_3(\sigma) = \frac{1}{(S_2^T)^2} (\sigma_{22} + \sigma_{33})^2 + \frac{1}{(S_{23}^F)^2} (\sigma_{23}^2 - \sigma_{22}\sigma_{33}) + \frac{1}{(S_{12}^F)^2} (\sigma_{12}^2 + \sigma_{13}^2) = 1$
Compressive Matrix $\sigma_{22} + \sigma_{33} < 0$	$F_4(\sigma) = \frac{1}{S_2^C} \left[\left(\frac{S_2^C}{2S_{23}^F} \right)^2 - 1 \right] (\sigma_{22} + \sigma_{33}) + \frac{1}{4(S_{23}^F)^2} (\sigma_{22} + \sigma_{33})^2 + \frac{1}{(S_{23}^F)^2} (\sigma_{23}^2 - \sigma_{22}\sigma_{33}) + \frac{1}{(S_{12}^F)^2} (\sigma_{12}^2 + \sigma_{13}^2) = 1$

$$S(d_1, d_2, d_3, d_4) = \begin{bmatrix} \frac{S_{11}}{1-d_1} & S_{12} & S_{13} & 0 & 0 & 0 \\ S_{12} & \frac{S_{22}}{1-d_2} & S_{23} & 0 & 0 & 0 \\ S_{13} & S_{23} & \frac{S_{33}}{1-d_2} & 0 & 0 & 0 \\ 0 & 0 & 0 & \frac{S_{44}}{1-d_3} & 0 & 0 \\ 0 & 0 & 0 & 0 & \frac{S_{55}}{1-d_3} & 0 \\ 0 & 0 & 0 & 0 & 0 & \frac{S_{66}}{1-d_4} \end{bmatrix} \quad (1)$$

Damage variables are used to scale elastic constants as a function of the failure indicators from the Hashin failure criteria. The relationship between f_1, f_2, f_3, f_4 and d_1, d_2, d_3, d_4 is described in Table 5. Each damage variable is controlled such that its value can only remain constant or increase, effectively eliminating material ‘healing’ during damage. It should be noted that the strength of each constituent material is considered constant, meaning that as failure indicators predict failure at material points, the strengths that are used for this prediction do not change with increasing damage.

Table 5. Damage variable definitions

Damage Mode	Damage Variable Value
Longitudinal Damage (fiber)	$d_1 = \alpha (\max \{f_1, f_2\})$
Transverse Damage (matrix)	$d_2 = \alpha (\max \{f_3, f_4\})$
Longitudinal Shear (combined)	$d_3 = 1 - (1 - d_1)(1 - d_2)$
Transverse Shear (combined)	$d_4 = d_3$

3.2. Damage Evolution Law

The relationship between failure indicators and damage variables defined in Table 5 introduces a damage evolution function $\alpha = \alpha(f)$. This damage evolution function describes the rate at which damage (material degradation) is assigned to each material point. Introducing instantaneous damage evolution results in a very brittle material response, whereas nonlinear damage evolution (exponential, power, etc) allows for a more progressive response during material failure. Both instantaneous and exponential damage evolution are considered in this progressive damage model, and are described in Equations 2 and 3, respectively.

$$\alpha(f) = \begin{cases} 0, & \text{if } f < 1 \\ d_{max}, & \text{otherwise} \end{cases} \quad (2)$$

Resin failure is assumed to be brittle and therefore an instantaneous damage law is applied. It is also assumed that there is some residual stiffness after failure, resulting a decision to use $d_{max} = 0.90$, meaning 10% of the original stiffness remains after failure. A maximum principal stress criteria was used to evaluate damage and failure in the matrix. Elements representing transversely isotropic impregnated tows are assigned an exponential damage evolution behavior, defined in Equation 3, where m is a material response parameter and e is the base of the natural logarithm. As m increases, the damage characteristics approach that of an instantaneous damage response.

$$\alpha(f) = d_{i \max} \left[1 - \exp\left(-\frac{f^m}{m e}\right) \right] \quad (3)$$

Equation 3 includes the maximum material degradation parameter $d_{i \max}$. The value of $d_{i \max}$ has been defined based on previous work by Tan and Perez and Camanho and Matthews [5, 16, 17]. Since, for an impregnated tow, damage variables d_3 and d_4 are functions of d_1 and d_2 , values for the maximum material degradation parameter need only be defined for $d_{1 \max}$ and $d_{2 \max}$. These parameters are separated for tensile and compressive failure modes, allowing for different residual (post-failure) stiffnesses at each material point depending upon the failure mode. Values used for $d_{1 \max}$ and $d_{2 \max}$ are shown in equations 4 and 5, respectively.

$$d_{1 \max} = \begin{cases} 0.93, & \text{if tension} \\ 0.80, & \text{if compression} \end{cases} \quad (4)$$

$$d_{2 \max} = \begin{cases} 0.86, & \text{if tension} \\ 0.60, & \text{if compression} \end{cases} \quad (5)$$

4. Results

The primary objective for this first-pass progressive damage model is to capture the onset and initial propagation of damage within the bolted joint of interest. A comparison between simulation-predicted failure modes and locations with experimental results is discussed in this section. Ref. [9] discusses the primary experimental failure modes at the onset of damage in a double-shear configuration. Observed failure modes include longitudinal warp tow compressive damage, weft tow compressive failure in the transverse direction and matrix cracking surrounding these tows within the bearing area. As bearing strain increases, the extent and severity of these failure modes was observed to increase and was eventually accompanied by late shear cracking and shear-out failures.

The extent of warp and weft tow damage at a considerable bearing strain is shown in Figure 2. Damage accumulates in both warp and weft tows in the bearing area. It was found that warp tows experienced longitudinal compressive damage along the bearing surface and transverse tow damage at the edges of the hole. Weft tows were found to primarily experience transverse compression along the bearing surface (aligned with the loading direction). While cracking propagated to the free surface of the bearing sample, fiber reinforcement was still intact, resulting in a zero-stiffness region in the stress-strain response. This simulation was terminated once the weft column along the bearing surface experienced complete material degradation. This also corresponds to the onset of shear-out type failures.

The value of the material response parameter m was varied to adjust the rate at which exponential damage is applied to the impregnated tow elements. For a material response parameter $m = 5$, the simulation-predicted bearing stress-strain response is shown in Figure 3 and is directly compared with experimental findings from Ref. [9]. Seen in the Figure, the predicted stress-strain response is similar to the experimental curve through the region of damage onset.

5. Conclusion

The non-linear behavior of a three-dimensional woven composite subjected to bearing stresses in a single-bolt, double-lap joint configuration was explored in this paper. Represented by a realistic as-

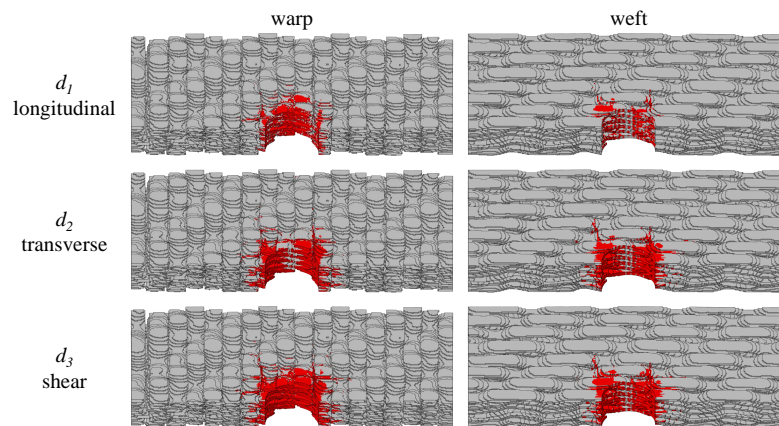


Figure 2. Cross-sectional cut of the mesoscale portion of the model showing the bearing surface and predicted warp and weft tow damage at 7.3% bearing strain for each failure mode. The loading direction aligns with the warp tows.

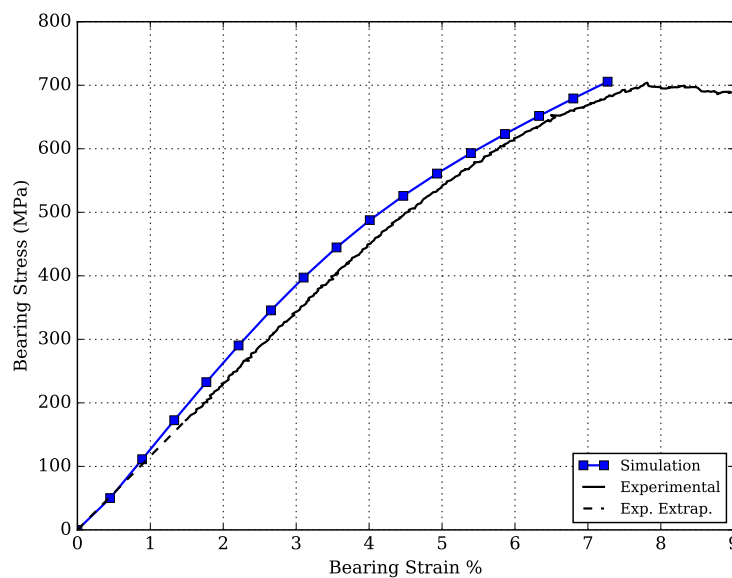


Figure 3. Simulation-predicted bearing stress-strain response compared with experimental findings for material response parameter $m = 5$. ‘Exp. Extrap.’ is a linear extrapolation from the start of the linear-elastic region used for bearing stiffness calculation back to the origin. This is included to eliminate the ‘strain correction’ region described in ASTM D5961 [8] as a combination of joint straightening, friction and translation due to hole clearance.

molded morphology, a mesoscale model was used to consider failure mechanisms in both impregnated tow and matrix material phases discretely. A combination of the well-established Hashin failure criteria, the Matzenmiller-Lubliner-Taylor damage model and an exponential damage evolution law was used to model the behavior of impregnated tows. Failure modes and mechanisms predicted by this first-pass progressive damage model were found to correlate well with experimental findings.

Excerpt from ISBN 978-3-00-053387-7

References

- [1] J Goering and M McClain. Recent developments in 3D woven pi preforms. In *American Society for Composites, 22nd Technical Conference*, 2007.
- [2] P Perugini, A Riccio, and F Scaramuzzino. Three-dimensional progressive damage analysis of composite joints. In *8th International Conference on Civil and Structural Engineering Computing, Paper*, 2001.
- [3] A Riccio and F Scaramuzzino. Influence of damage onset and propagation on the tensile structural behavior of protruding composite joints. In *4th GRACM Congress on Computation Mechanics GRACM*, pages 27–29, 2002.
- [4] Stepan V Lomov, Dmitry S Ivanov, Ignaas Verpoest, Masaru Zako, Tetsusei Kurashiki, Hiroaki Nakai, and Satoru Hirose. Meso-FE modelling of textile composites: Road map, data flow and algorithms. *Composites Science and Technology*, 67(9):1870–1891, 2007.
- [5] PP Camanho and FL Matthews. A progressive damage model for mechanically fastened joints in composite laminates. *Journal of Composite Materials*, 33(24):2248–2280, 1999.
- [6] MA McCarthy and CT McCarthy. Finite element analysis of effects of clearance on single shear composite bolted joints. *Plastics, Rubber and Composites*, 32(2):65–70, 2003.
- [7] Kyle C Warren, Roberto A Lopez-Anido, Senthil S Vel, and Harun H Bayraktar. Progressive failure analysis of three-dimensional woven carbon composites in single-bolt, double-shear bearing. *Composites Part B: Engineering*, 84:266–276, 2016.
- [8] ASTM International, West Conshohocken, PA. *ASTM Standard D5961, Standard Test Method for Bearing Response of Polymer Matrix Composite Laminates*, 2010.
- [9] KC Warren, RA Lopez-Anido, and J Goering. Behavior of three-dimensional woven carbon composites in single-bolt bearing. *Composite Structures*, 127:175–184, 2015.
- [10] KC Warren, RA Lopez-Anido, and J Goering. Experimental investigation of three-dimensional woven composites. *Composites Part A: Applied Science and Manufacturing*, 73:242–259, 2015.
- [11] *CYCOM PR 520 RTM Resin System, Cytec Engineered Materials*, 2012.
- [12] Zvi Hashin. Failure criteria for unidirectional fiber composites. *Journal of Applied Mechanics*, 47(2):329–334, 1980.
- [13] CT McCarthy, MA McCarthy, and VP Lawlor. Progressive damage analysis of multi-bolt composite joints with variable bolt-hole clearances. *Composites Part B: Engineering*, 36(4):290–305, 2005.
- [14] Chang-Li Hung and Fu-Kuo Chang. Bearing failure of bolted composite joints. Part II: model and verification. *Journal of Composite Materials*, 30(12):1359–1400, 1996.
- [15] A Matzenmiller, J Lubliner, and RL Taylor. A constitutive model for anisotropic damage in fiber-composites. *Mechanics of Materials*, 20(2):125–152, 1995.
- [16] Seng C Tan. A progressive failure model for composite laminates containing openings. *Journal of Composite Materials*, 25(5):556–577, 1991.
- [17] Seng C Tan and Jose Perez. Progressive failure of laminated composites with a hole under compressive loading. *Journal of Reinforced Plastics and Composites*, 12(10):1043–1057, 1993.